4-4-2005

Mechanism for spatial organization in quantum dot self-assembly

Da Gao
Michigan Technological University

Adam Kaczynski
Michigan Technological University

John A. Jaszczak
Michigan Technological University

AIP | Applied Physics Letters

Mechanism for spatial organization in quantum dot self-assembly

Da Gao, Adam Kaczynski, and John A. Jaszczak

Citation: Applied Physics Letters **86**, 133102 (2005); doi: 10.1063/1.1896090
View online: http://dx.doi.org/10.1063/1.1896090
View Table of Contents: http://scitation.aip.org/content/aip/journal/apl/86/13?ver=pdfcov
Published by the AIP Publishing

Mechanism for spatial organization in quantum dot self-assembly

Da Gao, Adam Kaczynski, and John A. Jaszczak[a)]
Department of Physics, Michigan Technological University, 1400 Townsend Drive, Houghton, Michigan 49931-1295

(Received 13 October 2004; accepted 15 February 2005; published online 21 March 2005)

Inspired by experimental observations of spatially ordered growth hillocks on the (001) surfaces of natural graphite crystals, a mechanism for spatial organization in quantum dot self-assembly is proposed. The regular arrangement of steps from a screw dislocation-generated growth spiral provides the overall template for such ordering. An ordered array of quantum dots may be formed or nucleated from impurities driven to the step corners by diffusion and by their interactions with the spiral's steps and kinks. Kinetic Monte Carlo simulation of a solid-on-solid model supports the feasibility of such a mechanism. © *2005 American Institute of Physics*. [DOI: 10.1063/1.1896090]

While many insights about the mechanisms for self-assembly of quantum dots (QDs) have been obtained,[1] useful mechanisms for controlling the spatial ordering of self-assembled quantum dots remain a challenge. In this letter we propose that the interactions of surface impurities with steps and kinks of a screw-dislocation-generated growth spiral could be a possible means of controlling the spatial arrangement of quantum dots during self-assembly.

The interaction of impurities with a growth spiral has been suggested as a possible mechanism for the formation of unusual surface topographies observed on the (001) surfaces of natural graphite crystals from Namibia.[2] Growth hillocks occur on these crystals at the corners of the steps of their growth spirals (Fig. 1). Although the scale of these features is quite large (tens of microns; see Ref. 2 for details), the proposed mechanism could also be effective in controlling QD self-assembly at the nanoscale using spiral growth steps emanating from screw dislocations.[3] Under appropriate conditions, to be explored below, we propose the following scenario: Adatom impurities on the crystal surface diffuse toward and stick to a regular array of advancing growth steps emanating from one or more screw dislocations terminating at a crystal surface. During growth of the host crystal, the steps advance by the motion of kinks, which drive impurities to move toward the corners of the steps. Diffusion of impurities on the terraces could also favor higher impurity concentrations at the corners. The increased impurity concentration at corners of the steps favors the formation of impurity clusters. Once such clusters form they would both pin the advancement of the steps at the corners leading to reentrant notches and eventually lead to hillock formation as subsequent growth might eventually bury the immobile impurity clusters.

We have developed an atomistic solid-on-solid (SOS) model of a (001) surface of a simple cubic crystal and carried out kinetic Monte Carlo (KMC) (Refs. 4, 5) simulations in order to investigate the hypothetical scenario outlined above. Each surface site could be a single host or impurity atom. While the number of impurities was fixed, host atoms could adsorb or evaporate. Both impurities and host atoms could diffuse to nearest-neighbor sites. However, impurities were forbidden to diffuse on top of other impurities. Monte Carlo moves were generated based on the rates of adsorption r_a, evaporation r_{ei}, and diffusion from surface site i to another surface site j $r_{i\to j}$, and were calculated following Ref. 6 as

$$r_a = v\,\exp\left(\frac{3\Phi_{11}}{k_BT}\right)\exp\left(\frac{\Delta\mu}{k_BT}\right), \tag{1}$$

$$r_{ei} = v\,\exp\left(\frac{\Delta E_i}{k_BT}\right), \tag{2}$$

$$r_{i\to j} = d_s(x_l/a)^2 r_{ei}, \quad l = 1,2, \tag{3}$$

where the surface vibration frequency $v = 10^{12}\ \mathrm{s}^{-1}$, k_B is the Boltzmann constant, T is the temperature, and $\Delta\mu$ is the chemical potential driving force for host atoms. Evaporation and diffusion rates depended on an energy barrier $\Delta E_i = m\Phi_{11} + n\Phi_{22} + p\Phi_{12}$, where m, n, $p = \{0,1,2,3,4,5\}$ represent the number of bonds of a given type formed with the surface atom at site i, and Φ_{11}, Φ_{22} and Φ_{12} are the nearest-neighbor bond energies for host–host, impurity–impurity, and host–impurity interactions, respectively. In Eq. (3), a is the lattice spacing, and x_l is the mean diffusion distance for host ($l=1$) and impurity atoms ($l=2$), respectively. The diffusion factor $d_s = 1$ for most surface atoms, but for impurity atoms bonded to steps, $d_s = \exp(-\Phi_{12}/k_BT)$, as an enhance-

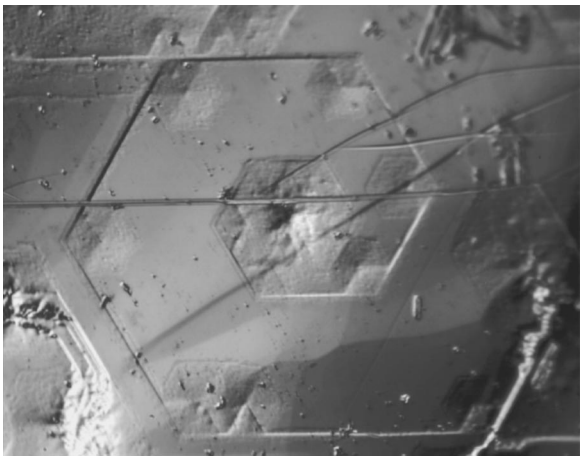

FIG. 1. Differential interference contrast optical photograph of a growth spiral (field of view $235 \times 185\ \mu$m) on the (001) surface of a naturally occurring graphite crystal (Ref. 2) from western Namibia with a regular arrangement of hexagonal growth hillocks at each corner of the growth spiral. All hillocks at the steps and corners of the growth spiral have 60° and 120° re-entrant notches, respectively.

[a)]Electronic mail: jaszczak@mtu.edu

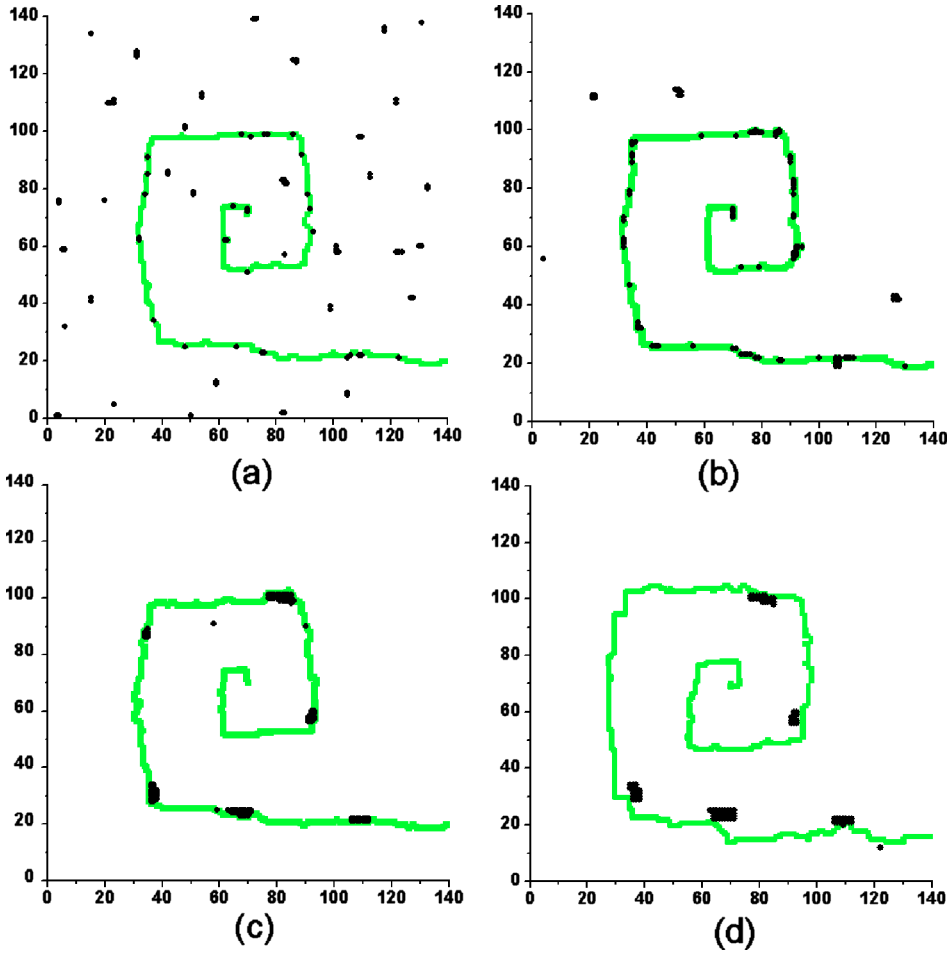

FIG. 2. (Color online) Comparison of surface morphologies just after (a) 1 MCS (2.8×10^{-8} s); (b) 10 MCS (9.4×10^{-6} s); (c) 150 MCS (1.3×10^{-2} s); and (d) 350 MCS (6.8×10^{-2} s) for a simulation of 100 impurities on a 141×141-site surface at $T=100$ K. The continuous curves are contours interpolated from surface height differences, and show the spiral growth step emanating from a central screw dislocation at each time. Black markers indicate the positions of the impurities.

ment to impurity diffusion along steps. A diffusion enhancement for host atoms at steps was not similarly implemented in order to save computational time.

A spiral step was grown on a surface with 141×141 sites with a single screw dislocation using boundary conditions as described in Ref. 7 at $T=100$ K and $\Delta\mu=5.0\ k_BT$. The surface was initially flat except for a straight unit-height step emanating from the dislocation and terminating at a reflective boundary. Under the same conditions, a crystal without a dislocation had a negligible growth rate. Time was monitored in terms of Monte Carlo Sweeps (MCS), where 1 MCS is accomplished when the number of Monte Carlo moves equals the number of surface sites, as well as in real time[4,5] (seconds). After 400 MCS (0.56 s) of initial growth, impurity atoms were randomly distributed on the surface, and the simulation continued at the same T and $\Delta\mu$ as before the impurities were added.

Bond energies and diffusion parameters were varied in order to study their effects on the surface topography. Using $x_l/a=1.0$ for host atoms, $x_l/a=0.01$ for impurities, and $\Phi_{11}=-0.0800$ eV, $\Phi_{22}=-0.0810$ eV, and $\Phi_{12}=-0.0425$ eV, the following dynamics were observed. After only 1 MCS, the impurities had already diffused to form small clusters (mostly dimers) as shown in Fig. 2(a). These small clusters eventually disappeared as individual impurities diffused to larger clusters and to the spiral growth steps [Fig. 2(b)]. Eventually, the impurities formed a small number of clusters (QDs) as shown in Figs. 2(c) and 2(d) just before they were laterally "buried" by the continual addition of host atoms to the growing spiral. Before becoming laterally buried, the QDs were typically located along steps or near the corners of the spiral.

The effects of the impurities on the overall growth rate are illustrated in Fig. 3. Initially (region I in Fig. 3) the impurities diffused on the terraces to form small clusters or attached to host atoms at the growth spiral steps. The overall growth rate was relatively slow [1.1 monolayers per second (ML/s)] in this region due to impurity "poisoning" of the steps and kinks.[8] As time progressed the impurities formed larger clusters, and some migrated to the step corners. One by one, the impurity clusters were buried laterally by surrounding host atoms. As impurities clustered and became buried, kink sites once again became available for growth, and the growth rate increased to approximately 1.7 ML/s (region II in Fig. 3). Finally, once all of the impurities became buried the growth rate increased to its maximum rate of 2.6 ML/s (region III in Fig. 3).

The surface dynamics was found to be very sensitive to the choice of parameters in Eqs. (1)–(3). The temperature and chemical potential values were selected to yield a growth spiral with several turns and well defined corners on a surface of reasonable size for the simulation. The bond energies were constrained to satisfy $(\Phi_{11}+\Phi_{22})/2-\Phi_{12}<0$, in order to favor the phase separation of impurities from the host crystal, yet Φ_{12} was maintained sufficiently negative to keep the impurities interacting with the steps. Making Φ_{22} stronger ($\leqslant-0.09$ eV) resulted in impurities forming large clusters which could become immobile even before reaching growth steps. Making Φ_{12} weaker resulted in increased impurity diffusion and a decreased tendency for the creation of

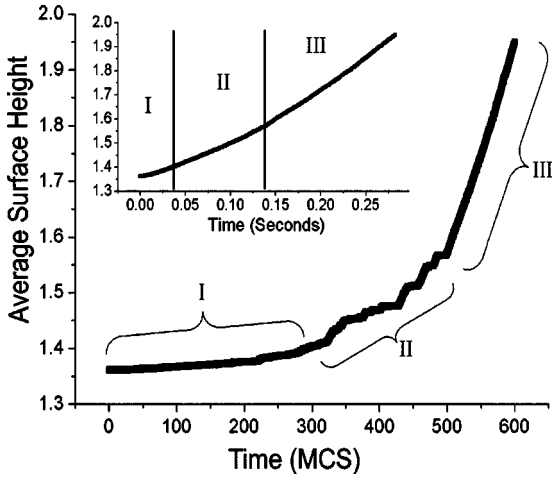

FIG. 3. Average surface height (in monolayers) of the surface as a function of time under the same conditions as in Fig. 2. The dynamics in region I were dominated by impurity diffusion on the terraces and at the steps. In region II impurities formed clusters and got partially buried laterally by host atoms, while in region III all impurities were laterally buried. The inset shows the change of the average surface height as a function of real time.

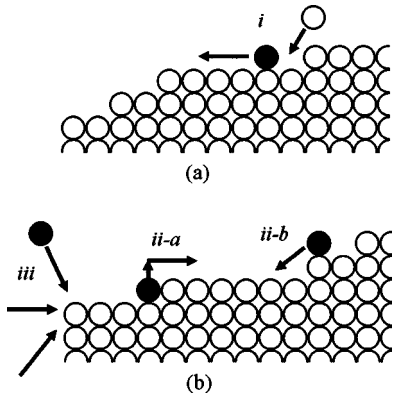

FIG. 4. Diagram viewed looking down at the topmost layer on the surface showing the three atomistic-level moves for mechanisms of self-assembly of quantum dots at spiral step corners. Open circles represent host atoms and filled circles represent impurities. A step corner is located at the left in both diagrams. (a) Mechanism *i* shows impurities driven to the corners by kink motion during host growth. (b) In mechanism *ii*, uphill diffusion [*ii-a*] is slower than downhill diffusion [*ii-b*] due to the higher activation energy in *ii-a*. Mechanism *iii* favors impurity segregation at the corners since corners have larger effective areas on the terraces from which to draw diffusing impurities.

impurity clusters. On the other hand, making Φ_{12} stronger ($\leqslant -0.07$ eV) caused the impurities to become buried too easily by the advancing growth steps. While it was straightforward to find parameters favoring diffusion of impurities to the steps, it was difficult to find parameters favoring their forming clusters at the steps, and particularly difficult to form clusters near the corners. Enhancing the impurity diffusion along the steps was found to be important, in that for simulations without the step diffusion enhancement factor d_s (but under otherwise identical conditions), impurities formed smaller clusters along the growth spiral steps and showed less tendency to form clusters at the step corners. Increasing the number of impurities increased the number of clusters on the steps and decreased the growth rate.

Studies of the variation of the above parameters and detailed observations of the morphological evolution as a function of time suggests that there are at least three possible mechanisms favoring the spatially-organized self-assembly of quantum dots in our simulations, which are illustrated in Fig. 4: (i) Effective "pushing" of impurities along steps toward corners by the advancement of kinks as the host crystal grows by the addition of host atoms at kink sites [move *i* in Fig. 4(a)]. Bond energies can be tuned to favor host atoms over impurities to bond at the kink sites. (ii) Net "downhill" diffusion[9] of impurities due to effective energy barriers to impurity migration to move "up" a kink [*ii-a* in Fig. 4(b)] as compared to moving "down" a kink toward a corner [*ii-b* in Fig. 4(b)]. Further neighbor interactions, Schwoebel-type barriers for atoms moving along steps near kinks, and explicit activation energies could further enhance this effect. (iii) Impurity adatoms on terraces would tend to diffuse toward corners more than to steps due to the "lightning rod effect" since corners have larger effective areas on the terraces from which to draw diffusing impurities [*iii* in Fig. 4(b)].

Our results suggest that the proposed mechanism of controlling the spatial organization of self-assembled quantum dots by using the interaction of impurities with regularly-spaced steps of dislocation-induced growth spirals is feasible, but careful tuning of growth conditions and interaction strengths may be necessary. More detailed models taking into account activation barriers, impurity strain effects, Schwoebel-type barriers, dimmer mobility, and larger system sizes could provide other means of testing and ultimately controlling the arrangement, size, uniformity, and shapes of quantum dots.[10] A practical implementation would require a regular array of screw dislocations to be generated in a material, which is also a nontrivial task. One possible method would be to first create a one-dimensional source of dislocations on a semiconductor surface by scratching or nanoindentation. Subsequent straining of the crystal can generate streams of dislocation pairs that move across the surface from the sources to form a two-dimensional array of dislocations intersecting the surface.[11]

The authors are grateful to John Rakovan, Steve Hackney, and Ed Nadgorny for helpful discussions. This work was supported in part by the National Science Foundation (Grant No. SES 0304439).

[1] K. Pohl, M. C. Bartelt, J. de la Figuera, N. C. Bartelt, J. Hrbek, and R. Q. Hwang, Nature (London) **397**, 238 (1999).
[2] J. Rakovan and J. A. Jaszczak, Am. Mineral. **87**, 17 (2002).
[3] S. Kodambaka, S. V. Khare, W. Swiech, K. Ohmori, I. Petrov, and J. E. Greene, Nature (London) **429**, 49 (2004).
[4] A. B. Bortz, M. H. Kalos, and J. L. Lebowitz, J. Comput. Phys. **17**, 10 (1975).
[5] S. Clarke, M. Wilby, and D. Vvedensky, Surf. Sci. **255**, 91 (1991).
[6] G. H. Gilmer and P. Bennema, J. Appl. Phys. **43**, 1347 (1972).
[7] R. H. Swendsen, P. J. Kortman, D. P. Landau, and H. Müller-Krumbhaar, J. Cryst. Growth **35**, 73 (1976).
[8] K. J. Davis, P. M. Dove, and J. J. De Yoreo, Science **290**, 1134 (2000).
[9] L. A. N. Amaral and J. Krug, Phys. Rev. E **55**, 7785 (1997).
[10] M. Kotrla, J. Krug, and P. Simlauer, Surf. Sci. **482–485**, 840 (2001).
[11] E. Nadgorny, *Dislocation Dynamics and Mechanical Properties of Crystals, Progress in Materials Science* (Pergamon, Oxford, 1988), Vol. 31, pp. 371–400, 434–468.